IMPACT OF DIRECTIONAL PROPERTIES ON THE RADIOMETRIC TEMPERATURE MEASUREMENT IN RAPID THERMAL PROCESSING

Y.H. Zhou, Y.J. Shen, and Z.M. Zhang[1]
Department of Mechanical Engineering, University of Florida
Gainesville, Florida 32611

B.K. Tsai and D.P. DeWitt
Optical Technology Division, National Institute of Standards and Technology
Gaithersburg, Maryland 20899

ABSTRACT

A quasi-Monte Carlo model has been developed to predict the effective emissivity for accurate radiometric temperature measurements in rapid thermal processing (RTP) furnaces. The hemispherical effective emissivities calculated from this Monte Carlo method agree with those calculated from the net-radiation method. The Monte Carlo method, however, can also be used to determine the directional effective emissivity and the true effective emissivity, which is needed to obtain the wafer temperature from the measured spectral radiance temperature by the lightpipe radiation thermometer (LPRT). If the wafer is not diffuse, the true effective emissivity may be quite different from the hemispherical emissivity, especially for specular wafers with emissivities less than 0.6. For the RTP system studied here, the largest effective emissivity is obtained with a numerical aperture of about 0.5.

KEY WORDS: effective emissivity; Monte Carlo method; radiometric temperature measurement; rapid thermal processing; RTP.

INTRODUCTION

Rapid thermal processing (RTP) has prominent applications in the new century due to the continuing advances in semiconductor technology [1]. RTP has been replacing batch furnaces in several critical manufacturing processes for integrated circuits. A significant challenge in the development of RTP technology is the accurate measurement and control of the wafer temperature. Because of the nature of fast response and non-intrusiveness, lightpipe radiation thermometers (LPRTs) are commonly used to monitor the wafer temperature during the process. One of the methods to reduce the measurement uncertainty caused by the emissivity variation and stray light is the usage of a cold reflective shield [2-4]. The effective emissivity must be precisely determined to correct the radiometer reading because LPRTs are normally calibrated against blackbodies.

Researchers at the University of Florida and National Institute of Standards and Technology (NIST) have developed effective emissivity models for RTP furnaces based on the net-radiation method [3-6]. The results showed that, with the highly reflective shield, the effective emissivity approaches one and is less sensitive to variations of the wafer emissivity.

[1] Corresponding author, zzhang@cimar.me.uf.edu

The guard ring and the guard tube have strong influence on the local effective emissivity of the wafer. Although the algorithm based on the net-radiation method is fast and convenient, only the hemispherical effective emissivity can be obtained. The strong temperature non-uniformity and the large property variation of the surfaces in a RTP furnace may cause significant directional dependence of the effective emissivity. The hemispherical effective emissivity may not be appropriate to use in practice, because the LPRT views the wafer in a small solid angle, usually much less than 2π sr.

A more complicated statistical approach, i.e., the Monte Carlo method, is the preferred choice to study the impact of the directional dependence of the properties on the radiometric temperature measurement. Earlier, Monte Carlo methods have been used to predict the effective emissivity of nearly isothermal cavities [7-9]. Howell [10] gave a comprehensive review on the applications of Monte Carlo methods in radiative heat transfer. Cole et al. [11] and Mazumder and Kersch [12] developed Monte Carlo models to study the radiative heat transfer in thermal processing. Recently, Adams et al. [13] used a Monte Carlo model to predict the effective emissivity and considered the effect of the bidirectional reflectivity distribution function (BRDF). Their ray-tracing algorithm was not very efficient and, for this reason, some simplifications had to be made in the modeling.

In the present paper, we describe a general Monte Carlo model for the study of radiative transfer in the lower chamber of RTP furnaces. Several definitions of the effective emissivity are described in detail. In addition to the hemispherical effective emissivity, the model can predict the distribution of the directional effective emissivity, the effective emissivity based on the spot-to-lightpipe geometry, and the effective emissivity based on the numerical aperture.

MODEL DEVELOPMENT

Figure 1 shows a schematic of the model for the lower chamber of RTP furnaces that employ a reflective shield and use LPRTs to monitor the wafer temperature. It is based on the NIST RTP tool [6]. The lower chamber is modeled as a cylindrical enclosure. The top surface is a silicon *wafer* with a coplanar *guard ring*, the bottom surface is the *shield* (a gold-coated, water-cooled copper plate), and the lateral surface is a platinum-coated quartz *guard tube*. The lightpipe, located at the center of the shield, views a small portion of the wafer (spot). There are four off-center holes in the shield that can accommodate other lightpipes. In the actual system (not shown in Fig. 1), the wafer is supported by three rods, whose length can be adjusted to vary the distance between the wafer and the shield. An array of quartz-halogen lamps heats the wafer from above.

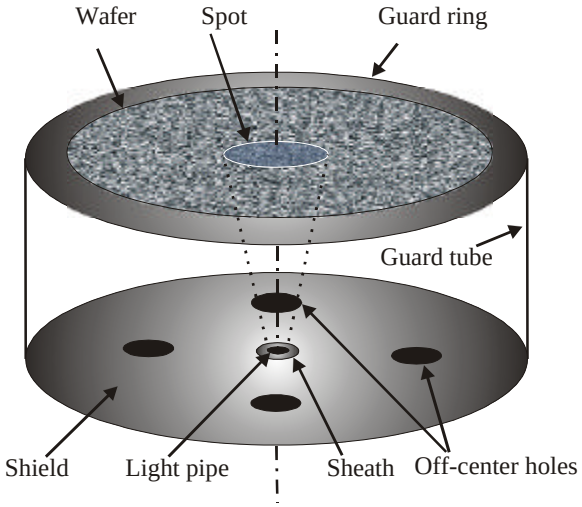

Figure 1. Schematic of the lower chamber model for RTP furnaces (not to scale).

The radius of the wafer is 100 mm and inner radius of the guard tube is 135 mm. In the enclosure analysis, it is assumed that the radius of the shield is 135 mm, and the inner and outer radii of the guard ring are 100 mm and 135 mm, respectively. The radii of the sapphire lightpipe and the sheath are approximately 1 mm and 2 mm, respectively. The off-center holes are located at 54 mm from the center of the shield with a radius of 3.5 mm. The distance between the wafer and the shield L is typically 12.5 mm. The radius of the spot is experimentally determined to be $r_s = r_p + L/3$, where r_s and

r_p are the radius of the spot and that of the lightpipe, respectively. The temperature of the wafer is much higher than that of the other surfaces. The shield is highly reflective and the lightpipe tip, sheath, and holes are almost black. The operating wavelength of the LPRT is 0.955 μm.

The Net-Radiation Method

A brief review of the net-radiation method is presented in this section to facilitate the discussion of various definitions of the effective emissivity. For an opaque, diffusely emitting surface, the (hemispherical) reflectivity can be adequately represented by a combination of a diffuse component and a specular component, then [14]:

$$\rho_\lambda = \rho_\lambda^d + \rho_\lambda^s = 1 - \varepsilon_\lambda \qquad (1)$$

where superscripts *d* and *s* denote respectively the diffuse and the specular components and ε_λ is the spectral emissivity.

For an enclosure consisting of *N* such surfaces, the (diffuse) spectral radiosity J_λ for the i^{th} surface is defined as

$$J_{\lambda,i} = \varepsilon_{\lambda,i} E_{\lambda b,i} + \rho_{\lambda,i}^d H_{\lambda,i} \qquad (2)$$

where $E_{\lambda b}$ is Planck's blackbody emissive power, and $H_{\lambda,i}$ is the spectral irradiation that can be expressed as

$$H_{\lambda,i} = \sum_{j=1}^{N} J_{\lambda,j} F_{i-j}^s \qquad (3)$$

where F_{i-j}^s is the specular view factor between surface A_i and surface A_j. Equations (2) and (3) can be combined to eliminate $H_{\lambda,i}$. The resulting *N* linear algebraic equations can be solved for the radiosities if the surface temperatures are given [5]. The irradiation for each surface can then be calculated using Eq. (3).

The (spectral) effective emissivity of the wafer can be defined as the ratio of the radiant energy leaving the wafer by emission and reflection to that of a blackbody at the same temperature, viz.,

$$\varepsilon_{eff,w} = [\varepsilon_{\lambda,w} E_{\lambda b,w} + (1 - \varepsilon_{\lambda,w}) H_{\lambda,w}] / E_{\lambda b,w} \qquad (4)$$

where subscript w stands for the wafer. The effective emissivity from Eq. (4) depends on the position on the wafer and therefore it is a local property. Another way of defining the effective emissivity is to consider the receiving surface (such as the lightpipe in Fig. 1). In this case,

$$\varepsilon_{eff,p} = H_{\lambda,p} / E_{\lambda b,w} \qquad (5)$$

It can be viewed as the spectral irradiation at the lightpipe tip divided by the spectral irradiation in a blackbody surrounding at the wafer temperature.

Either definition gives a hemispherical effective emissivity, whereas the directional distribution of the irradiation is in general not diffuse. The lightpipe can only view a limited solid angle due to the detector optics. It is common to use the *numerical aperture* of the lightpipe, defined as

$$NA = \sin\theta_h \qquad (6)$$

where θ_h is the half cone angle. The directional distribution of the irradiation may influence the thermometer reading. Moreover, if more surfaces are non-diffuse, the specular view factor will be difficult to obtain. While the net-radiation method is conceptually simple and

convenient for programming, it cannot deal with complicated situations.

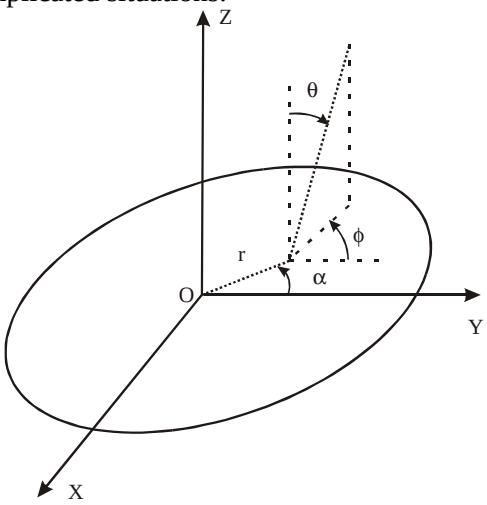

Figure 2. Illustration of the position and direction variables on the top and bottom surfaces.

The Monte Carlo Method

In the Monte Carlo model, the procedure begins by emitting ray bundles at random from each surface. The number of bundles and the energy per bundle are determined from the surface area and the spectral emissive power, which in turn depends on the surface temperature and emissivity. All surfaces are assumed opaque and diffusely emitting. In order to obtain the local effective emissivity, the wafer, the guard ring, and the shield are further divided into smaller concentric rings. On each ring, the properties and temperature are assumed uniform, except for the ring on the shield that contains the four off-center holes. In this ring, the properties of the holes are evaluated separately from the other part of the ring. As shown in Figure 2, the position is defined by a radius r on the top and bottom surfaces (or a height h on the guard tube) and a circumferential angle α. The direction is defined by a polar angle θ and an azimuthal angle φ. Four random numbers between 0 and 1 are generated to determine the position and direction of emission for each bundle, namely R_r (or R_h), R_α, R_θ, and R_φ. The radius of the outgoing point on each ring is calculated by

$$r = \sqrt{R_r (r_i^2 - r_{i-1}^2) + r_{i-1}^2} \qquad (7a)$$

where r_{i-1} and r_i are correspondingly the inner and outer radii of the i^{th} ring. If the emission is from the guard tube, the height is given by

$$h = R_h L \qquad (7b)$$

where L is the distance between the wafer and the shield. The circumferential angle is

$$\alpha = 2\pi R_\alpha \qquad (8)$$

Because the emission is diffuse, the directional angles are calculated by

$$\theta = \sin^{-1}\sqrt{R_\theta} \quad \text{and} \quad \varphi = 2\pi R_\varphi \qquad (9)$$

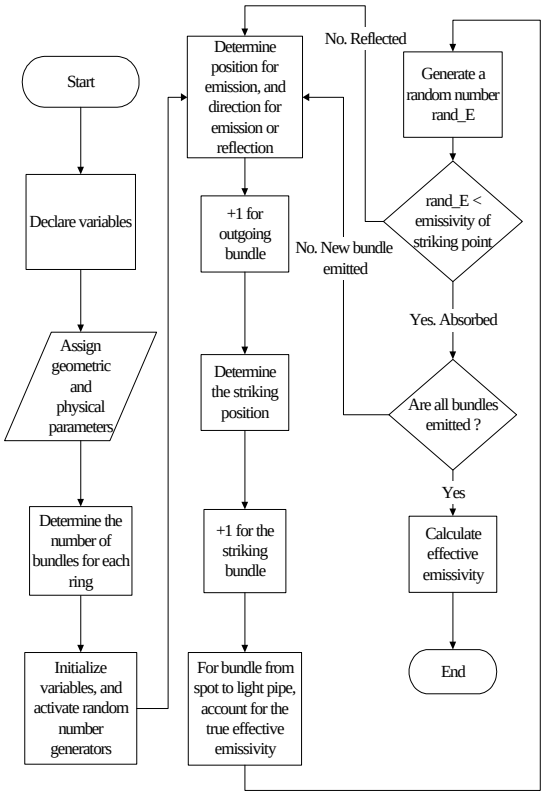

Figure 3. Flowchart of the Monte Carlo procedure.

After each ray bundle is emitted, it will be traced in the enclosure until it is absorbed. The flowchart for the Monte Carlo simulation procedure is shown in Fig. 3. For rays originating from the top or bottom surfaces, the arriving point (r_2, α_2) on the opposite surface can be obtained from the starting point (r_1, α_1) and direction (θ_1, φ_1) by:

$$\begin{cases} r_2 \cos\alpha_2 = L \tan\theta_1 \cos\varphi_1 + r_1 \cos\alpha_1 \\ r_2 \sin\alpha_2 = L \tan\theta_1 \sin\varphi_1 + r_1 \sin\alpha_1 \end{cases} \quad (10)$$

For the case in which the calculated r_2 is greater than r_s (the radius of the shield or guard tube), the ray will strike the guard tube. The height h_2 is obtained by replacing r_2 with r_s and L with h_2 (or $L - h_2$ if the emission is from the top surface) in Eq. (10). For rays originating from the guard tube, the following expressions are used to determine the arriving position:

$$\begin{cases} r_2 \cos\alpha_2 = r_s \cos\alpha_1 + b \cot\varphi_1 \sin\alpha_1 \\ \qquad\qquad - b \cos\alpha_1 / (\tan\theta_1 \sin\varphi_1) \\ r_2 \sin\alpha_2 = r_s \sin\alpha_1 - b \cot\varphi_1 \cos\alpha_1 \\ \qquad\qquad - b \sin\alpha_1 / (\tan\theta_1 \sin\varphi_1) \end{cases} \quad (11)$$

where b is the displacement in the z direction.

After the arriving point is obtained, one more random number is required to determine whether this bundle is absorbed or reflected. The reflection is considered, in general, to include a specular component and a diffuse component. If the reflection is specular, the reflection direction is opposite to the incident direction. If the reflection is diffuse, two more random numbers are needed and the reflection direction is calculated in the same way as for the emission, i.e., according to Eq. (9).

The local effective emissivity of the wafer can be calculated by

$$\varepsilon_{eff,w} = \frac{N_{emitted,w} + N_{reflected,w}}{N_{emitted,bb}} \quad (12)$$

The numerator is the sum of emitted and reflected bundles from a ring, and the denominator is the number of bundles that would be emitted by a blackbody at the same temperature and area. Equation (12) gives a hemispherical effective emissivity. Because only the bundles reaching the lightpipe from the spot contribute to the radiometer reading, another effective emissivity, called *true effective emissivity*, can be defined,

$$\varepsilon_{eff,s-p} = \frac{N_{s-p}}{N_{s-p,bb}} \quad (13)$$

The numerator is the number of bundles (emitted and reflected) from the spot to the lightpipe tip, and the denominator is the number of bundles from the spot to the lightpipe if the spot were a blackbody. The denominator can be directly calculated from the view factor and the blackbody emissive power.

The effective emissivity based on the ray bundles that strike the lightpipe can be expressed as

$$\varepsilon_{eff,p} = \frac{N_{strike}}{N_{strike,bb}} \quad (14)$$

The denominator is the number of bundles that strike the lightpipe tip from a blackbody surrounding at the wafer temperature. This definition can also be extended to give the directional effective emissivity by considering only bundles within a small interval about θ for $0 \le \varphi < 2\pi$. Furthermore, because the lightpipe collects radiation within a certain numerical aperture, another effective emissivity may be defined based on the half angle of the acceptance cone:

$$\varepsilon_{eff,\theta_h} = \frac{N_{strike\ within\ \theta_h}}{N_{strike\ within\ \theta_h, bb}} \qquad (15)$$

Equation (15) gives the hemispherical effective emissivity when $\theta_h = 90°$ (i.e., *NA* = 1). Because the radius of the lightpipe is much smaller than the radius of the spot, the results of Eq. (13) and Eq. (15) are nearly the same. Either Eq. (13) or Eq. (15) gives the true effective emissivity value that should be used in the working equation of LPRTs. The emissivities defined in this section are all spectral, though the word spectral has been omitted.

Methods for Random Number Generation

Because the Monte Carlo method is a statistical method, for complicated problems, the choice of algorithm for the random number generation is very important. The functions implemented in most programming languages are based on the *linear congruential generator* [15,16]. The simplest pseudo-random number sequence can be obtained by dividing an integer sequence by the modulus *m* (often the largest integer in the computer):

$$R_j = I_j / m \qquad (16a)$$

The integer sequence is generated from

$$I_j = aI_{j-1} + c \,(\text{mod } m),\ j = 1, 2, \ldots \qquad (16b)$$

where *a* and *c* are positive integers, which can be selected so that the period of the sequence approaches *m*. The "mod *m*" in the parentheses of Eq. (16b) is a mathematical notation that indicates that I_j is subtracted by *m* as many times as needed to yield a positive integer less than *m*. The random numbers obtained from Eq. (16a) are in the domain [0, 1]. An arbitrary initial value may be assigned as I_0, which is called the seed. This random number sequence satisfies the test for pseudo-random numbers and, if *a*, *c*, and *m* are carefully chosen, any seed choice is as good as any other in a one-dimensional space. However, in a *k*-dimensional space ($k > 1$), the sequences are no longer independent between the dimensions.

For the simulation of the RTP radiation process, four random numbers are required to determine the position and direction of emission from the surfaces. Those random numbers should be independent. Therefore, the *quasi-random sequences* are employed in the present study [15,16]. The corresponding Monte Carlo method is often called the quasi-Monte Carlo method. The scheme of this kind of sequence can be conceptually interpreted by the Halton's sequence. In one dimension, the j^{th} number I_j in the sequence is obtained by the following two steps: (i) Write *j* as a number in base *d* where *d* is some prime number; (ii) Reverse the digits and put a radix point in front of the number obtained previously. In a space of *k* dimensions, each component is taken from the Halton's sequence with a different prime base. The advantage is that the successive points will fill in the gaps in the previously generated distribution. In our calculation, the advanced procedure of the Antonov-Saleev variant of the Sobol's sequence is employed [15]. Figure 4 shows the comparison of the point distributions on the wafer spot between the quasi-random sequences and the linear congruential generator ($I_0 = 7$) in the Monte Carlo model. Obviously, the quasi-random number sequences yield more uniformly distributed points. It has been shown that the linear congruential random number generator may produce erroneous results for the true effective emissivity [17]. In the quasi-Monte Carlo model described in the present paper, the quasi-random sequences are used for the location and direction of the emitted ray bundles and an improved linear congruential generator is used to obtain additional random numbers for the absorption and reflection.

RESULTS AND DISCUSSION

In the calculation, the temperature of the wafer is set to 800 °C and the temperature of all other surfaces is set to 25 °C. The reflectivity of

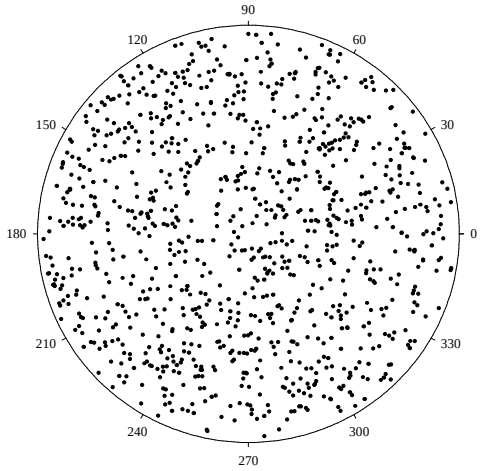

(a) the linear congruential generator (I_0 = 7)

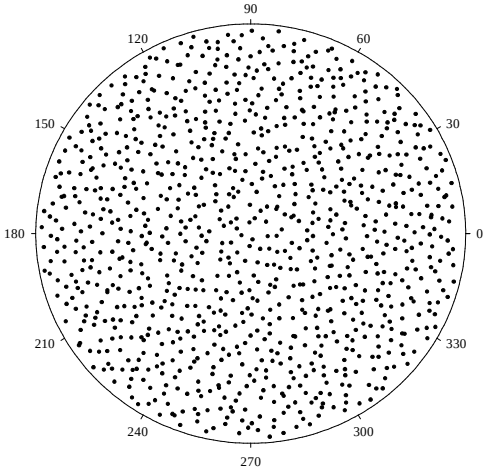

(b) the quasi-random sequence

Figure 4. Point distributions on the spot for different random number generators.

the shield is 0.993. The emissivity of the guard ring and guard tube is 0.1. The emissivity of the lightpipe, sheath, and off-center holes is assumed to be the same as sapphire, which is 0.925. The emissivity of the wafer is 0.651 at 800 °C. Because the wafer emissivity varies for different batches or even during the thermal processing, it is important to know the influence of the wafer emissivity on the effective emissivity. The emissivity of the wafer is therefore taken as a variable. In general, the reflectivity can have a diffuse component and a specular component. For the Monte Carlo simulation results presented here, the guard ring and the guard tube are assumed to reflect diffusely, while the shield (including the lightpipe, sheath, and off-center holes) is assumed specular. The wafer is specular in most cases and may have both specular and diffuse components in some cases. The Monte Carlo simulation obtains the hemispherical and true effective emissivities in the same run. It takes about 2 million bundles from the spot for the results of the true effective emissivity to converge within ±0.003. The total number of emitted bundles (almost all of them are from the wafer) is 1.1 billion and it takes about 8 hours for each run on a 600 MHz Pentium III computer. That is to say that the average time for each ray bundle is about 30 μs. Because the off-center holes are far away from the center, their influence on the effective emissivities at the center is negligibly small. Nevertheless, the capability of including off-center holes is a unique feature of this Monte Carlo program.

Figure 5 compares the true effective emissivity and the hemispherical emissivity calculated with the quasi-Monte Carlo method for a specular wafer versus the wafer emissivity. The hemispherical values predicted from the net-radiation method are also shown for comparison. Due to the limitations of the net-radiation method, the shield is assumed diffuse and the guard ring is assumed specular with the same reflectivity as that of the wafer. The use of diffuse shield slightly over-predicts the hemispherical effective emissivity, and the use of the wafer reflectivity for the guard ring slightly under-predicts the effective emissivity. The calculated hemispherical emissivity based on the spot is consistent between the Monte Carlo method and the net-radiation method. The hemispherical effective emissivity based on the lightpipe is consistently lower; this can be understood by the fact that the irradiation on the lightpipe includes direct contributions of the cold guard ring and guard tube. It is noteworthy

that, as the wafer emissivity is changed from 0.3 to 0.8, the true effective emissivity changes from 0.945 to 0.990, whereas the hemispherical effective emissivity (from the Monte Carlo model) will vary from 0.853 to 0.987. This suggests that the true effective emissivity is less sensitive to the wafer emissivity, a desired feature for the radiometric temperature measurement. For wafer emissivities less than 0.6, the difference between the true effective emissivity and the hemispherical effective emissivity can be significant.

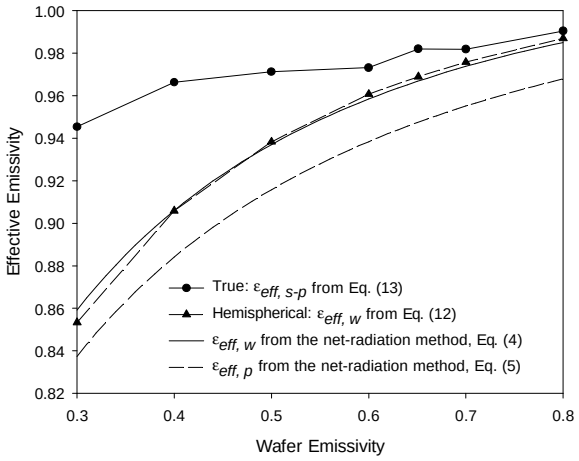

Figure 5. The relationship between the effective emissivity and wafer emissivity.

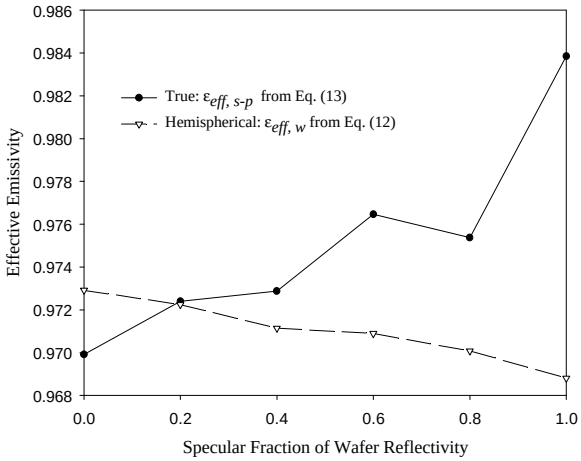

Figure 6. Effective emissivity vs. specular fraction of the wafer reflectivity.

The influence of the specular fraction of the wafer is shown in Fig. 6, where the emissivity of the wafer is 0.651. The specular fraction is defined as $\rho_\lambda^s / \rho_\lambda$, see Eq. (1). In principle, the true effective emissivity should be the same as that of the hemispherical one for a diffuse wafer. The difference of about 0.003 is caused by the uncertainty in computing the true effective emissivity because the view factor between the spot and the lightpipe is very small. The hemispherical effective emissivity is the maximum if the wafer reflection is diffuse and decreases slightly (about 0.004 from the completely diffuse to the completely specular). On the contrary, the true effective emissivity increases as the specular ratio increases and reaches the maximum with specular reflection. The true effective emissivity changes for about 0.014 from the completely diffuse to the completely specular. The difference between the true effective emissivity and the hemispherical emissivity for a specular wafer is about 0.015, corresponding to a 1 °C difference in LPRT reading at temperature 1000 K for a bandpass around 1 μm. The difference in the true effective emissivity between specular wafer and diffuse wafer would be larger for lower wafer emissivities. Although the reflection of actual surfaces may be better represented by the BRDFs, Adams et al. [13] showed that the predicted effective emissivity with measured BRDFs lies somewhere between completely diffuse and completely specular cases.

The angular distribution of the directional effective emissivity at the lightpipe is shown in Fig. 7 for wafer emissivities of 0.3 and 0.651, where the interval in θ is 3° in the calculation. The directional effective emissivity is close to that of the wafer at $\theta \to 0°$. This is because of the high emissivity of the lightpipe and sheath coupled with specular reflections; that is, there is little or no enhancement in the normal effective emissivity. The directional effective emissivity increases with θ, reaches a maximum, and then decreases as θ further increases. The decrease at large angles is caused by the cold guard ring and guard tube. If the striking bundles follow the *Lambert's cosine law*, the directional effective emissivity should be a constant for all polar

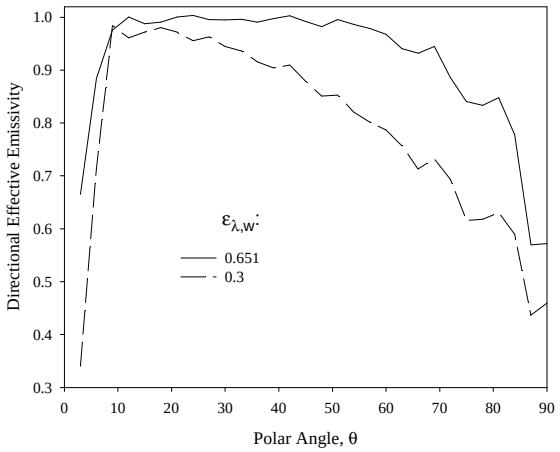

Figure 7. Angular distribution of the directional effective emissivity at the lightpipe for different wafer emissivities.

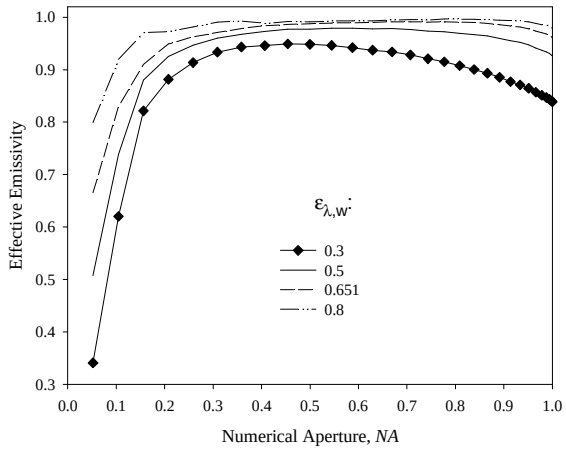

Figure 8. The effective emissivity $\varepsilon_{eff,\theta_h}$ calculated from Eq. (15) vs. the numerical aperture.

angles. Figure 7 shows that the directional effective emissivity varies sharply with the polar angle, especially with small wafer emissivities. This is the reason why the reverse method in which the rays are emitted from the lightpipe (presumably following the Lambert's cosine law) and collected at the wafer would yield an error for nearly specular wafers [13].

The effective emissivity calculated from Eq. (15) versus the numerical aperture of the lightpipe is shown in Fig. 8. The half angle of the spot viewed from the center of the lightpipe is 22.6° (*NA* = 0.384), the resulted $\varepsilon_{eff,\theta_h}$ is almost the same as the true effective emissivity calculated from Eq. (13). Similar to Fig. 7, $\varepsilon_{eff,\theta_h}$ increases first and then decreases as the numerical aperture increases. There exists a numerical aperture where the effective emissivity is the greatest. The half cone angle corresponding to the maximum $\varepsilon_{eff,\theta_h}$ is about 25° for $\varepsilon_{\lambda,w} = 0.3$ and increases to 50° for $\varepsilon_{\lambda,w} = 0.8$. A choice of the half cone angle close to 30° (*NA* = 0.5) is recommended because, at large wafer emissivities, the effect of the numerical aperture on the effective emissivity is not so strong.

SUMMARY AND CONCLUSIONS

A Monte Carlo model has been developed to analyze the radiative transfer in the lower chamber of RTP furnaces. The uniqueness of the model presented here includes the use of quasi-random sequences, the addition of off-center holes, and the definition of the true effective emissivity that should be used to correct the reading of the radiation thermometers. The results show that for non-diffuse wafers, the true effective emissivity may deviate from the hemispherical value due to the directional dependence of the incoming radiation on the lightpipe. The deviation is even greater for specular wafers with an emissivity less than 0.6. There exists an optimized numerical aperture that yields the highest effective emissivity. For the conditions studied here, a numerical aperture of 0.5 (i.e., half cone angle of 30°) is recommended.

ACKNOWLEDGMENTS

This work has been supported by the NIST Office of Microelectronics Program and the National Science Foundation (CTS-9875441).

REFERENCES

[1] P.J. Timans, Materials Science in Semiconductor Processing, vol. 1 (1998), p. 169.

[2] D.P. DeWitt, F.Y. Sorrell, and J.K. Elliott, "Temperature Measurement Issues in Rapid Thermal Processing," in Mat. Res. Soc. Symp. Proc., vol. 470 (1997), p.3.

[3] F. Rosa, Y.H. Zhou, Z.M. Zhang, D.P. DeWitt, and B.K. Tsai, "Modeling Chamber Radiation Effects on Radiometric Temperature Measurement in Rapid Thermal Processing," in the Electrochemical Society Proceedings, vol. 99-10 (1999), p. 419.

[4] B.K. Tsai and D.P. DeWitt, "ITS-90 Calibration of Radiometers Using Wire/Thin-Film Thermocouples in the NIST RTP Tool: Effective Emissivity Modeling," in Proc. 7th Int. Conf. Advanced Thermal Processing of Semiconductors – RTP'99, 1999, p. 125.

[5] Z.M. Zhang and Y.H. Zhou, "An Effective Emissivity Model for Rapid Thermal Processing Using the Net-Radiation Method," Fourteenth Symposium on Thermophysical Properties, Boulder, CO, June 2000; submitted to International Journal of Thermophysics.

[6] C.W. Meyer, D.W. Allen, D.P. DeWitt, K.G. Kreider, F.L. Lovas, and B.K. Tsai, "ITS-90 Calibration of Radiometers Using Wire/thin-film Thermocouples in the NIST RTP Tool: Experimental Procedures and Results," in RTP'99, 1999, p. 136.

[7] A. Ono, Journal of the Optical Society of America, vol. 70 (1980), p. 547.

[8] Z. Chu, J. Dai, and B.E. Bedford, Temperature, Its Measurement and Control in Science and Industry, AIP, 1992, vol. 6 (1992), p. 907.

[9] V.I. Sapritsky and A.V. Prokhorov, Metrologia, vol. 29 (1992), p. 9.

[10] J.R. Howell, Journal of Heat Transfer, vol. 120 (1998), p. 547.

[11] J.V. Cole, K.L. Knutson, and K.F. Jensen, "Monte Carlo Simulation of Radiative Heat Transfer in Rapid Thermal Processing (RTP) Systems," in Mat. Res. Soc. Symp. Proc., vol. 342 (1994), p.425.

[12] S. Mazumder and A. Kersch, "A Fast Monte Carlo Scheme for Thermal Radiation in Semiconductor Processing Applications," Numerical Heat Transfer, Part B, vol. 37 (2000), p. 185.

[13] B. Adams, A. Hunter, M. Yam, and B. Peuse, "Determining the Uncertainty of Wafer Temperature Measurements Induced by Variations in the Optical Properties of Common Semiconductor Materials," in Proceedings of 197th Meeting of the Electrochemical Society, Ontario, Canada, May 2000.

[14] M.F. Modest, Radiative Heat Transfer, McGraw-Hill, New York, 1993.

[15] W.H. Press, S.A. Teukolsky, W.T. Vetterling, and B.P. Flannery, Numerical Recipes in Fortran, 2nd ed., Cambridge University Press, Cambridge, UK, 1992, Chap. 7.

[16] S. Tezuka, Uniform Random Numbers: Theory and Practice, Kluwer Academic Publishers, Boston, MA, 1995.

[17] Y.H. Zhou, Y.J. Shen, Z.M. Zhang, B.K. Tsai, and D.P. DeWitt, "Monte Carlo Simulation for Radiometric Temperature Measurement in Rapid Thermal Processing," to be published in the Proceedings of the International Mechanical Engineering Congress and Exposition, Orlando, FL, Nov. 2000.